THE AMERICAN SOCIETY OF MECHANICAL ENGINEERS
345 E. 47th St., New York, N.Y. 10017

95-GT-3

HEAT TRANSFER AND FILM COOLING EFFECTIVENESS IN A LINEAR AIRFOIL CASCADE

N. Abuaf, R. Bunker
Corporate Research & Development
General Electric Company
Schenectady, NY

C.P. Lee
GE Aircraft Engines
General Electric Company
Cincinnati, OH

ABSTRACT

A warm (315 C) wind tunnel test facility equipped with a linear cascade of film cooled vane airfoils was used in the simultaneous determination of the local gas side heat transfer coefficients and the adiabatic film cooling effectiveness. The test rig can be operated in either a steady-state or a transient mode. The steady-state operation provides adiabatic film cooling effectiveness values while the transient mode generates data for the determination of the local heat transfer coefficients from the temperature-time variations and of the film effectiveness from the steady wall temperatures within the same aero-thermal environment. The linear cascade consists of five airfoils. The 14% cascade inlet free stream turbulence intensity is generated by a perforated plate, positioned upstream of the airfoil leading edge. For the first transient tests, five cylinders having roughly the same blockage as the initial 20% axial chord of the airfoils were used. The cylinder stagnation point heat transfer coefficients compare well with values calculated from correlations. Static pressure distributions measured over an instrumented airfoil agree with inviscid predictions. Heat transfer coefficients and adiabatic film cooling effectiveness results were obtained with a smooth airfoil having three separate film injection locations, two along the suction side, and the third one covering the leading edge showerhead region. Near the film injection locations, the heat transfer coefficients increase with the blowing film. At the termination of the film cooled airfoil tests, the film holes were plugged and heat transfer tests were conducted with non-film cooled airfoils. These results agree with boundary layer code predictions.

NOMENCLATURE

a	Constant = $h_f / \rho l c_p$
c_p	Stainless steel specific heat
ρ_c / ρ_g	Density ratio
g	Gravitational acceleration
h_f	Local heat transfer coefficient
J	Conversion factor
l	Airfoil wall thickness
m	Blowing ratio = $\rho_c U_c / \rho_g U_g$
Nu_{cyl}	Nusselt number based on cylinder diameter
Nu_{cyl}	Cylinder stagnation point Nusselt Number (Equation 4)
P	Local static pressure
Pr	Prandtl number
P_{stag}	Cascade inlet stagnation pressure
Re_D	Reynolds number based on cylinder diameter
Re	Reynolds number based on cascade inlet conditions and airfoil chord length
t	Time
T_{aw}	Adiabatic wall temperature
T_{cav}	Coolant feed cavity temperature
T_{co}	Coolant hole exit temperature
T_{rec}	Recovery temperature
Tu	Turbulence intensity
$T_w(steady\ state)$	Wall steady state temperature reached at end of transient
$T_w(initial)$	Initial wall temperature at onset of transient
$T_w(t)$	Wall temperature at time (t) of transient
U_c	Local film coolant hole exit velocity
U_g	Local air side velocity at film injection point
V_g	Free stream air inlet velocity

Presented at the International Gas Turbine and Aeroengine Congress & Exposition
Houston, Texas - June 5-8, 1995
This paper has been accepted for publication in the Transactions of the ASME
Discussion of it will be accepted at ASME Headquarters until September 30, 1995

Greek Symbols

η	Film cooling effectiveness
ρ	Stainless steel density
ρ_c	Local film coolant hole exit density
ρ_g	Local air side density at film injection location

1. INTRODUCTION

Advances in turbine performance over the past few decades have resulted from acquiring detailed information in each of the multi-disciplined efforts required for efficient turbine design and operation. With respect to the thermal design of turbines, and particularly the hot gas path components of the high pressure turbine, researchers have steadily obtained increased knowledge of both external and internal heat transfer. Aided by advances in instrumentation, data acquisition, computational capabilities, and new experimental methodologies, more and more of the specific factors affecting the thermo-physics are being investigated. This applies to localized regions of the turbine, such as interaction of film cooling jets with the mainstream gas and the surfaces as well as to the more global situations of passage and interstage flow and heat transfer. As designs approach stoichiometric turbine inlet conditions, obtaining such information under conditions which properly model the appropriate non-dimensional operating parameters, becomes of increasing importance.

In lieu of the extreme expense and difficulty of experimentation under actual turbine operating conditions, most research has utilized wind tunnels, cascades and turbine rigs that operate with reduced pressures and temperatures, and non-reacting gases. In the case of vane and blade heat transfer, a significant level of effort has been expended over the past 25 years by many researchers. This effort has increased in the last several years, such that many facilities are now operating to determine heat transfer distributions on airfoils with various conditions of film cooling, coolant to-gas density ratios, blowing parameters, inlet flow turbulence intensities, Reynolds numbers, unsteadiness, etc. These facilities incorporate several differing methodologies, most of which result in a few limitations being imposed on the character and usefulness of the information obtained. For film cooled airfoils, it is desired to obtain both local heat transfer coefficients, and local adiabatic wall temperatures, within the same aero-thermal fluid and surface conditions.

Airfoil cascades generally operate under either steady-state or transient conditions. Steady-state cascades have been reported in recent experiments, which use a number of different methods. The cascades of Nirmalan and Hylton (1990) and Dullenkopf et al. (1991) utilized internally cooled airfoils, sufficiently instrumented with thermocouples, to determine the external heat transfer coefficients by finite element analysis. While this method is capable of obtaining heat transfer coefficients, under conditions of film cooling (e.g. Nirmalan and Hylton), to obtain the adiabatic film effectiveness, several experiments have to be run at different coolant temperatures. Cascade tests of Takeishi et al. (1990), Mehendale and Han (1992), and Ou et al. (1993) have used airfoils made of insulator materials, with surface mounted thin-foil heaters, having thermocouples imbedded or tack-welded behind the heaters. This method is capable of obtaining both heat transfer coefficients and film effectiveness, but must utilize two separate tests to do so, with differing thermal boundary conditions. Also, due to the materials typically used, such tests generally are limited in the operation temperatures (coolant-to-gas density ratio) and pressure (Reynolds Numbers) levels of the coolant and gas sides. In similar tests, liquid crystals have been used by Schobeiri et al. (1991), and Ou and Han (1992), to provide the surface temperature indication. Here also, the liquid crystals limit the range of temperatures which may be investigated and thus can not model the engine coolant-to-gas density ratios of around 2 unless a heavy gas is used as the coolant medium. The methodology employed by Liu and Rodi (1992) seeks to obtain a constant temperature surface via controlled heaters and temperature sensor feedback, and uses "hot-film" sensors to determine the local heat transfer coefficients without film cooling. Takeishi et al. (1992) used the mass transfer analogy with CO_2 injectant, under both stationary and rotational conditions, to determine film effectiveness locally. Thin-walled airfoils of metal, with imbedded thermocouples and internal insulation have been used by Takeishi et al. (1990), and in earlier tests of Lander et al. (1972), to obtain film effectiveness distributions for various film cooling configurations.

Several transient methodologies have been used to obtain heat transfer characteristics, with the particularly attractive feature of reducing costly experimental test times associated with the many hours of steady-state operation, especially for larger turbine rigs. Many researchers are now using Isentropic Light Piston Compression Tube facilities including Camci and Arts (1990, 1991), Arts and Lapidus (1992), Jones et al. (1978), Harasgama and Wedlake (1991). In these test rigs, airfoils made of machinable ceramic (Macor), or coated with a layer of ceramic, are instrumented with thin film gages on the exterior surface. The short duration of the test obtains a period of steady conditions as the compressed gas is expanded through the rig. Employing one-dimensional, semi-infinite conduction analysis of the surface yields the heat transfer coefficients. Short duration blow-down facilities, such as those of Guenette et al. (1989) and Haldeman et al. (1992), Abhari and Epstein (1992) are designed for the testing of entire turbine stages, or even high pressure and low pressure turbines together. Running to fully scaled engine parameters, these rigs must utilize actual or slave engine hardware. Fast response surface heat flux gages are used to determine the heat transfer coefficients, both instantaneous and averaged quantities locally. A method using very short duration tests have been demonstrated by Dunn and Stoddard (1979), and used for many turbine rig experiments such as those of Dunn et al. (1992). This method employs a shock tube facility to provide compressed gas with negligible heating of the turbine, thus reducing conduction effects. Here too, fast response surface gages determine the instantaneous heat transfer coefficients, all based upon turbine inlet temperature. The methodology of Vedula and Metzger (1991) requires two indications of surface temperature at the same point in space, but at differing times within one transient test (or two indications from two tests of essentially identical conditions). These researchers utilized Plexiglas substrates

coated with liquid crystals, and one-dimensional semi-infinite conduction modeling, to simultaneously determine both heat transfer coefficients and film effectiveness values locally, based upon the local reference temperatures. This method is limited in the test pressure and temperature levels, imposed by substrate material and by liquid crystals, and thus can not fully model engine dimesionless parameters. Finally, the cascade experiments by Lander et al. (1972) determined heat transfer coefficients from the transient heating of airfoils which were suddenly exposed to a convecting fluid of known conditions. These tests utilized two cascades, one to set flow conditions, and one to quickly shuttle into the flow. Thin-walled metal airfoils with imbedded thermocouples were used to obtain the temperature-time history of the surface at many locations.

The objectives of the present work were to build a transient test facility, similar to Lander et al., which will be able to provide both heat transfer coefficients and film cooling effectiveness values in linear airfoil cascades under pressure and temperature conditions which can simulate engine non-dimensional parameters.

2. TEST FACILITY

Apparatus

The transient facility presented in Figure 1 consists of the inlet components; the main air feed line, the inlet flow straightening section, and the containment box with an elevator carrying two identical cascade sections. The first cascade section (the dummy) is used to set the flow rates and the second cascade section has airfoils instrumented with pressure taps or imbedded thermocouples. The exit components consist of the exhaust section with a back pressure control valve, the system by-pass piping, the secondary film air cooling lines and the auxiliary air cooling lines for the elevator bearing and the containment box. The primary air is supplied by a Joy rotary compressor capable of providing air flow rates up to 4.53 kg/s at pressures up to 30 atmospheres and maximum preheat temperatures of 510 C. The flow straightening components upstream of the cascade consist of several sections transitioning the 15.24 cm diameter circular feed line into a rectangular inlet section for the linear cascade. Perforated plates are placed between the inter-connecting flanges at several sections of the test rig. The flow inlet section to the linear cascade included a flow converging section with elliptically shaped walls. The fiberglass insulated flow straightening section was enclosed in a 60.9 cm pipe. This enclosure, which is kept at a pressure close to the flow pressure, prevents the straightening section from experiencing large pressure differentials across its side walls. The containment box is 99.6 cm long, 24.6 cm wide and 96.5 cm high, and is manufactured from six heavy plates which can withstand the test pressures. The top wall of the box was used to provide all the penetrations for the cooling air feed lines. The secondary cooling air is supplied by a second compressor (the Worthington) which is capable of supplying 1.8 kg/s at pressures up to 30 atmospheres. A chiller installed between the film cooling cavity supply lines and the box permitted the control of the cooling air temperatures to perform

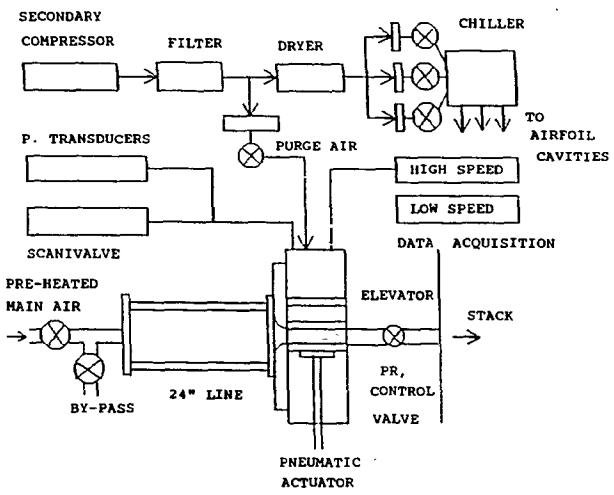

FIGURE 1. Schematic of test facility.

tests with coolant-to-main air density ratios of around 2. Three secondary air feed lines were provided to supply air to three airfoil film cooling cavities. The film cooling air was first passed through a filter and a drier before going into the air chiller. All the relevant air flow rates were measured with instrumented thin-plate orifices. The elevator was connected to the shaft of a pneumatic cylinder, at the bottom box wall, which was used for raising and lowering the elevator thus controlling the air flow to pass through the dummy or the instrumented cascade section.

The test rig instrumentation consists of flow temperature and pressure monitoring devices and the data acquisition system. For the present facility, there were two different sets of data acquisition requirements. For static tests, the data were collected at a slow pace over a relatively long period of time (every ten seconds over many hours). For dynamic tests, in addition to the steady state flow information, data were collected quickly over a short time period. Thirteen hundred data points for each of forty thermocouples were recorded during the initial 60 seconds of the transient During the first ten seconds the scan rate is set to 50 readings per second, during the next twenty seconds the scan rate is 25 readings per second, and during the last thirty seconds the scan rate is 10 readings per second.

Procedure

For the transient tests performed to obtain the heat transfer and film cooling effectiveness results, the following procedure was followed; i) with the elevator in the lower position, the main air flow conditions were set with the instrumented cascade in the flow field, ii) the auxiliary cooling air flows were adjusted, iii) the elevator was moved to the up position, transferring the flow to the "dummy cascade," iv) the secondary film cooling flows were adjusted for each active film cavity, v) the data acquisition was programmed for a dynamic test, vi) a transient test was initiated and conducted by actuating the pneumatic cylinder, moving the elevator down and exposing the instrumented

cascade to the main air flow, vii) the transient data was transferred to the main computer for future analysis, viii) steady state data were collected before and after the transient test to check the flow conditions.

To analyze the transient data and convert the temperature information into a local heat transfer coefficient, the lumped parameter equation derived by Lander, Fish and Suo (1972) was used. This equation represents a thin-walled section energy balance having negligible radiation and conduction losses, including the net lateral conduction within the wall and the conduction through the thermocouple leads. The lumped parameter approximation is usually valid for small values of the Biot number, defined as ($Bi = h_f l / k$). A curve fitting program was used to fit an exponential curve to the data.

$$\frac{T_w(steadystate) - T_w(t)}{T_w(steadystate) - T_w(initial)} = e^{-at} \tag{1}$$

Here $T_w(steadystate)$ corresponds to the local steady state temperature of the metal wall at the end of the transient, $T_w(initial)$ is the metal wall temperature at time zero and $T_w(t)$ is the temperature data recorded by the high speed data acquisition system at time t. The exponential constant a calculated by a curve fitting program was then used to calculate the local heat transfer coefficient, h_f, based on the temperature difference between the final and initial values of the temperatures.

$$a = \frac{h_f}{\rho \, l c_p} \tag{2}$$

In this expression ρ is the stainless steel density, c_p is the specific heat, and l is the wall thickness (0.165 cm).

The film effectiveness was calculated from;

$$\eta = \frac{T_{rec} - T_{aw}}{T_{rec} - T_{co}} \tag{3}$$

In this equation T_{aw} is the wall temperature measured at the end of the transient test when steady conditions are reached, T_{co} is the coolant exit temperature. The local recovery temperature, T_{rec} is calculated using a typical Mach number distribution taken from the cascade static pressure distribution results with a recovery factor of 0.88. Since one Mach number distribution was used for each series of tests having a given air flow rate, there may be slight errors in T_{rec}, near the trailing edge, due to variations in test-to-test pressure ratios and varying coolant addition amounts.

Using the method of Kline and McClintock (1953) for single sample experimental uncertainties, and considering the data acquisition standard deviations for the performed tests, the single sample uncertainties of the inlet gas, film coolant cavity, and adiabatic wall temperatures were estimated to be 1.5, 1.1, and 1.7 C respectively. The free stream velocity ranges from 0 to 274 m/s. Using a one percent as the uncertainty in the free stream velocity, the recovery temperature uncertainty is about 1.6 C. Then, taking the coolant exit temperature to be the cavity temperature, and using representative worst case temperature differences, the uncertainty in film effectiveness is plus/minus 0.01. Depending upon the film effectiveness local level, this represents from 1.5 percent to 17 percent uncertainty. The temperature difference between the recovery and coolant exit temperature is the controlling factor in this uncertainty. The uncertainty in the heat transfer coefficients measured with the transient method was calculated to be 8 percent for a typical test codition.

3. PRELIMINARY TESTS

For the transient tests, it was important to determine the elevator moving times between the up and down positions and compare the time scales involved with the thermal transient response time of the airfoil wall thermocouples. The travel time of the elevator under its own weight is around 0.2 seconds. The drop times are reduced to 0.1 seconds and to 0.07 seconds when the pneumatic cylinder is driven by 3.4 or 6.8 atmosphere pressures. This time scale of 0.1 second related to the motion of the elevator, is small when compared to the thermal transient test time which is usually of the order of tens of seconds.

Air velocity distributions were measured at five locations at the flow area in the flange downstream of the smooth elliptic converging section. The five traverse locations were chosen to be symmetrical with respect to the centerline of the passage. The velocity distributions were measured with a traversing Cobra probe while the flow discharged directly to atmosphere. The air flow was set to 0.47 kg/s, which provided a Reynolds Number of 146,150 based on the cascade inlet conditions and the airfoil chord length. The average mass velocity was 22.6 m/s. The average of the velocity distributions, measured at each one of the five traverse locations, were within five percent of the mass flow velocity.

Axial velocity profiles, head loss coefficients, and streamwise turbulence intensities and their decay downstream of a perforated plate, similar to the one used in the present tests upstream of the cascade inlet, were experimentally determined in a separate wind tunnel with hot wire anemometry. The perforated plate used had 0.63 cm diameter holes on 0.95 cm centers and a plate thickness of 0.32 cm, providing an open flow area of 42 %. The results showed that i) this specific perforated plate produced high turbulence intensities that decayed as a function of distance downstream of the plate, ii) the turbulence decayed to a constant value as a function of inlet Reynolds number. For the Reynolds numbers range of 90,000 to 180,000, a 14 % turbulence occurred at about 5 cm from the plate which is typical of the distance between the perforated plate and the airfoil leading edge.

4. CYLINDER IN CROSS FLOW

Tests were first conducted with cylinders in cross flow to record data with a basic configuration which has been studied extensively. A schematic of the test section with the cylinders in cross flow is presented in Figure 2. The test rig consisted of

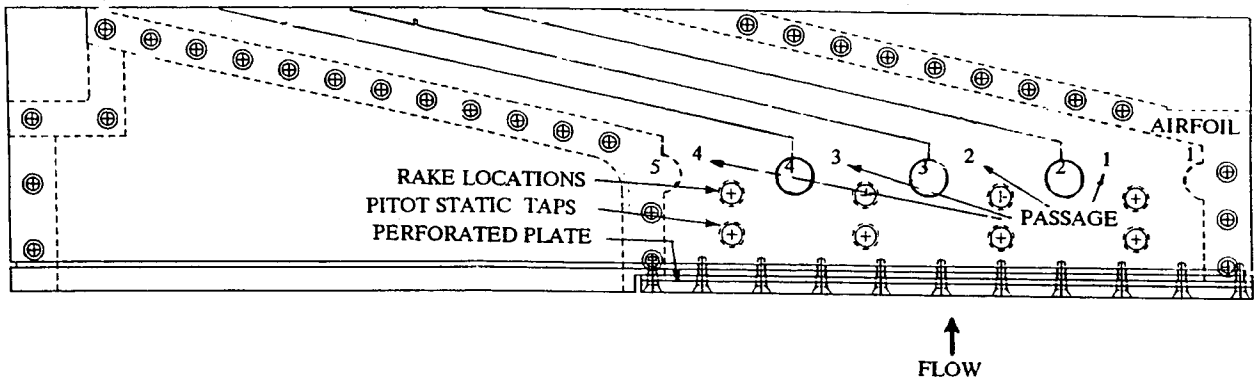

FIGURE 2. Schematic of the test section with cylinders in cross flow.

three hollow cylinders, shown as 2, 3 and 4 (1.587 cm in diameter, 0.165 cm wall thickness), and two half solid cylinders (1 and 5) forming a portion of the two side walls. The dimensions are representative of the airfoil leading edge flow blockage and wall thicknesses. The cylinders were positioned at a distance of 7.11 cm center-to-center. The side walls turning the flow at the exit region were straight. To evenly divide the flow between the four passages, side walls made out thin sheet metal were added downstream of each cylinder.

Two hollow center cylinders were prepared for data recording. The first one had a pressure tap at the stagnation point. The second instrumented one had a 0.051 cm thermocouple imbedded into a groove along the stagnation line. Both the pressure tap and the sensing point of the thermocouple were located at the center of the flow passage.

Flow velocity distributions were measured at the center of each of the four flow passages designated as 1 to 4 in Figure 2. The flow velocities at the center of each passage were measured by means of a cobra probe with the local static pressure for each passage being measured through a tap hole located 2.2 cm upstream of the probe. On the average the ratio of the cobra probe velocities to the mass average flow velocities is 1.03 and show a standard deviation of plus/minus ten percent. These velocity distributions showed that the inlet air flow was uniformly distributed among the four flow passages.

The transient heat transfer tests were conducted with the cylinder at air flow rates varying from 0.53 to 1.81 kg/s. Figure 3.a depicts the transient temperature data (solid line) as a function of time for a period of 60 seconds at the air flow rate of 0.53 kg/s, corresponding to a cylinder Reynolds number of 20700 . The initial cylinder wall temperature was 66 C and the final steady state temperature was 132.8 C which corresponds to the air temperature. Figure 3.b represents the transient temperature data (solid line) recorded at the higher flow rate of 1.81 kg/s, corresponding to a cylinder Reynolds number of 66530. The cylinder initial temperature in this case was 68 C and the final steady state temperature was 174 C. The open squares connected with a dashed line presented in Figures 3.a and 3.b correspond to the data fit obtained with the curve fit program.

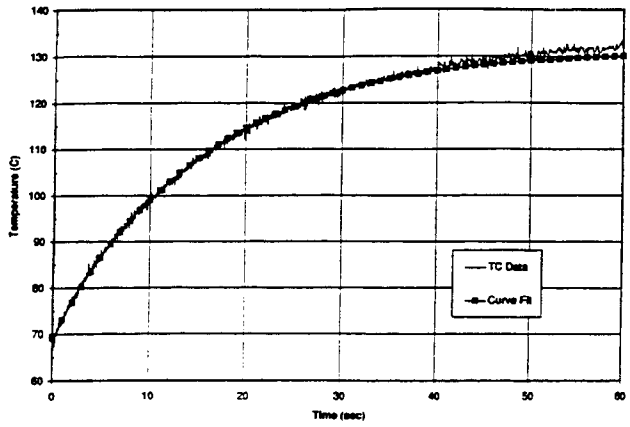

FIGURE 3a. Variation of stagnation point temperature with time for a transient test conducted at an air flow rate of 0.53 Kg/s, comparison with curve fit (squares).

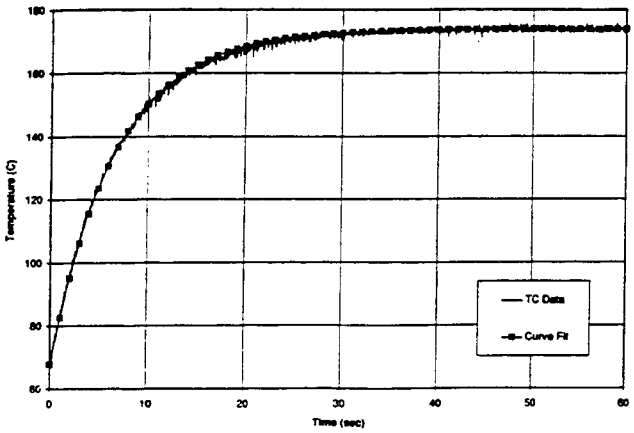

FIGURE 3b. Variation of stagnation point temperature with time for a transient test conducted at an air flow rate of 1.81 Kg/s, comparison with curve fit (squares).

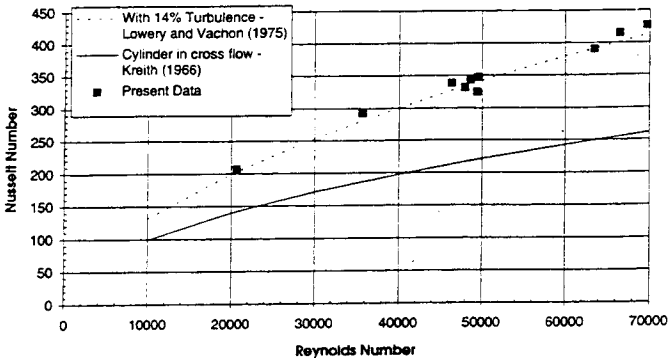

FIGURE 4. Comparison of cylinder stagnation point Nusselt Numbers data (solid diamonds) with cylinder in cross flow correlation (Kreith [1966]) and Lowery and Vachon's correlation [1975] accounting for turbulence effects.

The Nusselt numbers (based on cylinder diameter) calculated from the stagnation point heat transfer results are plotted as solid squares in Figure 4 as a function of the cylinder Reynolds numbers. On the same figure we have also plotted as a solid line the classical cylinder in cross flow stagnation point correlation (Kreith, 1966)

$$Nu_{cyl} = 1.14 \mathrm{Re}_D^{0.5} \mathrm{Pr}^{0.4} \tag{4}$$

The dashed line depicted in the same Figure represents the stagnation point heat transfer correlation presented by Lowery and Vachon (1975) which includes the effect of the free stream turbulence intensity.

$$\frac{\overline{Nu}}{\sqrt{\mathrm{Re}_D}} = 1.01 + 2.624\left[\frac{Tu\sqrt{\mathrm{Re}_D}}{100}\right] - 3.07\left[\frac{Tu\sqrt{\mathrm{Re}_D}}{100}\right]^2 \tag{5}$$

The experimental results agree quite satisfactorily with the cylinder stagnation point Nusselt number predictions with a free stream turbulence intensity of 14 percent.

5. LINEAR AIRFOIL CASCADE TESTS

The schematic of the cascade geometry is shown in Figure 5. The cascade has four flow passages and five smooth airfoils, counting the contoured side walls. The three center airfoils are removable and interchangeable, and are the instrumented ones. The lower end wall has seven static pressure taps as indicated, to monitor cascade inlet and exit pressures. The upper end wall has eight taps which may be used for pressure or temperature instrumentation rakes. The cascade inlet was provided with a turbulence generation grid providing a turbulence intensity of 14

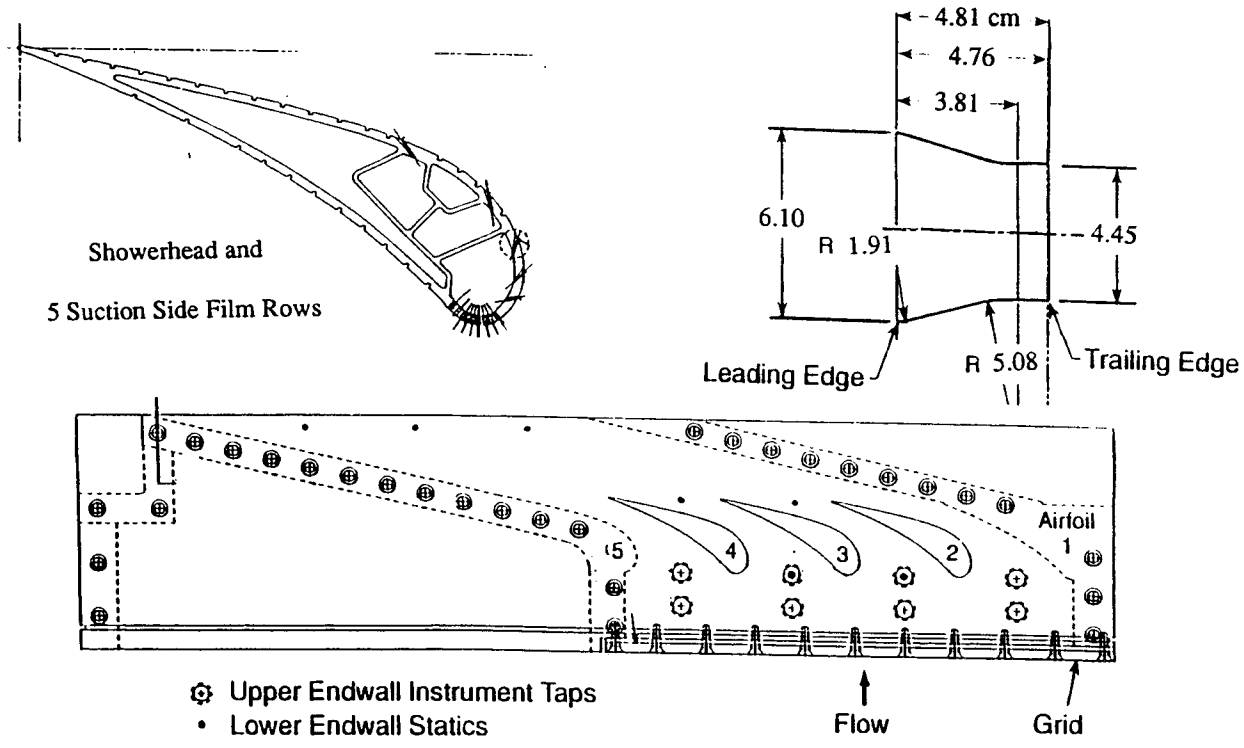

FIGURE 5. Schematic of the cascade test section, and Instrumented cascade airfoil configuration with thermocouple locations, film cooling holes and three film feed cavities.

percent at the leading edge plane. The flow path is convergent to simulate real nozzle passage geometries and the contraction is depicted in the insert of Figure 5. Three airfoils were instrumented with static pressure taps. One had static pressure taps all along the suction and pressure surfaces while the other two had pressure taps only along the suction or the pressure sides. During pressure distribution testing, the three airfoils were installed providing static pressures for the middle two flow passages. The static pressure taps are spaced 0.63 cm apart, beginning at the stagnation point of each airfoil. Airfoils 2 and 4 remain in the cascade for all testing. Figure 5 also shows the thermocouple locations for the specific airfoil configuration with three film cavities feeding fourteen rows of film cooling holes, nine in the shower head region plus five along the suction side.

First velocity distributions were measured at the center of each of the four cascade passages by a rake of seven Pitot tubes which were positioned at a distance of 6.35 cm upstream of the leading edge of the airfoils and at the center of each passage. With an air flow rate of 4.4 kg/s, an inlet pressure of 8.43 atm and temperature of 207 C, the average flow velocities of passages 1, 2, 3, and 4 were measured to be 30.2, 39.0, 36.9, 42.3 m/s respectively. The average flow velocity corresponds to 40.5 m/s. Passage 1 has a lower flow than 4, while passages 2 and 3 which surround the test airfoil appear to have flows close to the average. The throat widths of each passage were measured with a telescope gage and found that passage 1 had a smaller throat than passage 4. The air temperature distributions at the same four center passage locations were also measured with seven sensor thermocouple probes and found to be uniform with a maximum deviation of 0.8 percent.

To calculate the Mach number distributions along the centerline airfoil, static pressure distribution measurements were performed with the pressure instrumented airfoil for two flow rates. Static pressure distributions were also measured along the pressure side of Airfoil 2 and suction side of Airfoil 4, during the tests and found to agree with the center airfoil distributions. The Mach number distributions calculated from the pressure distributions for two Reynolds Numbers of 338,000 and 517,000 (mass flow 1.9 and 2.8 Kg/s) are presented in Figure 6. In the same Figure the calculated Mach numbers are compared with the predicted Mach number distributions for two cascade pressure ratios of 1.36 and 1.57. These pressure ratios correspond to the pressure ratios expected without and with film addition. The measured Mach number values are scattered within the two expected limits. The objective of these static pressure measurements was to show that all tests were performed under similar flow conditions, i.e. different Reynolds numbers but similar Mach number distributions.

The center airfoil was then replaced with the thermocouple instrumented one to conduct transient heat transfer tests. At the completion of the runs with film injection a series of tests was conducted to measure the local heat transfer coefficient distributions with no film injection and closed film holes. For these experiments all the film cooling holes were plugged with silicon RTV and the surface wiped as smooth as possible. Figures 7 and 8 depict the local heat transfer coefficients obtained for the pressure and suction sides (plugged holes) as a function of two

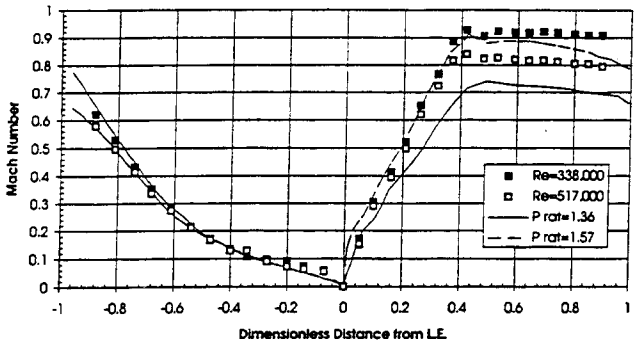

FIGURE 6. Plot of Mach number distributions as a function of distance from leading edge. Pressure side (negative x-axis), suction side (positive x-axis). Comparison with inviscid code Mach number predictions for two cascade pressure ratios of 1.36 and 1.57.

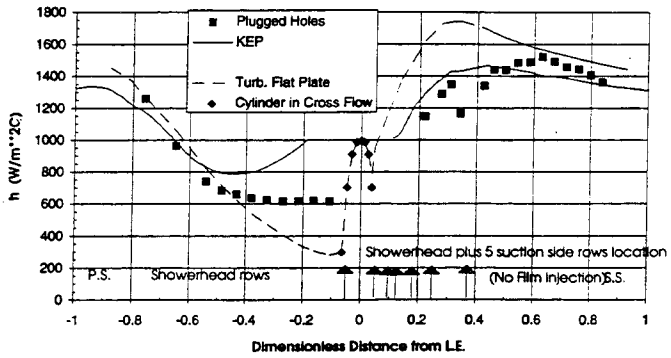

FIGURE 7. Comparison of heat transfer coefficients measured with the transient technique at an air Reynolds Number of 338,000 with plugged film holes versus the cylinder in cross flow and turbulent flat plate predictions and the boundary layer code (KEP) calculations.

Reynolds Numbers, 338,000 and 517,000 (mass flow rates 1.9 and 2.8 kg/s) with an inlet turbulence intensity of 14%. The heat transfer coefficients calculated from a cylinder in cross flow and turbulent flat plate correlations for the specific flow conditions and Mach number distributions are also presented. On the same Figures, we also present the heat transfer coefficients calculated from a boundary layer code with a k-ε turbulence model (KEP) for the same flow conditions and the Mach number distributions (Zerkle and Lounsbury, 1989). The KEP program is a modified version of the original STANX code. KEP uses a low Reynolds Number k-epsilon turbulence model while STANX solved the boundary layer equations using a hybrid turbulence model (mixing length model coupled with a one equation turbulence

model). The KEP code was tested by Zerkle and Lounsbury (1989) for the prediction of laminar and turbulent heat transfer and transition in flat plates. The same authors used the KEP program to predict heat transfer for vanes in a linear cascade and for rotating blades in a turbine test facility. In addition to the free stream turbulence intensity and flow acceleration, KEP also models the effect of surface curvature and surface roughness. The comparison shows that the heat transfer coefficients measured along the pressure side are lower than the predictions for a dimensionless distance larger than 0.5 and lie between the two predictions for shorter distances. On the other hand the suction side heat transfer coefficients are relatively flat along the surface, and lower than the turbulent flat plate predictions but closer to the boundary layer code calculations. Since the present film cooling row configuration had most of the film cooling holes along the leading edge showerhead region and along the suction side of the airfoil, the disturbance of the RTV plugged film cooling rows on the measured heat transfer coefficients is not known. The dip in the heat transfer coefficients observed near the fourth thermocouple (located at 4.09 cm from the leading edge stagnation point along the suction side), we believe is due to such an effect since this region is where the last row of film cooling holes are positioned, in addition to conduction losses due to the cavity ribs near this specific thermocouple.

Figure 8 also presents the heat transfer coefficients obtained with the transient method at a flow rate of 2.8 kg/s and an inlet turbulence intensity of 14 percent with film injection through all three film cavities. The shower head film had density ratios of around 2.0 and blowing ratios of 1.5 to 2.7 based on approach gas velocity and density, while suction side film rows had density ratios of 1.8 to 2.0 with blowing ratios of 1.2 to 1.4 based on local gas velocities and densities. The heat transfer coefficients along the pressure side show an increase in the local values due to the film injection at the leading edge which is being swept towards the pressure surface. The suction side heat transfer coefficients also show significant increases due to the film injection. The largest enhancement in the heat transfer coefficients is observed at the first thermocouple locations along the suction side. For the heat transfer coefficients investigated, the wall Biot numbers ranged between 0.06 and 0.23.

The steady state wall temperature distributions obtained at the end of the transient are plotted in Figure 9. Since the walls are not truly adiabatic, conduction corrections were required to adjust the measured wall temperatures. In regions where the walls are essentially one-dimensional and well insulated, these corrections are minor. But in more complex regions, such as near film holes, these corrections required more detailed analysis.

The individual coolant film row blowing ratios were calculated by using measurements of the cavity mass flow rates, cavity air pressures and temperatures, measured exit static pressures (Mach number distribution), and film hole discharge coefficients. The hole mass flow rates were used to estimate the coolant temperature rise through the film holes, taking into account entry and roughness effects on internal hole heat transfer. The resulting film exit temperatures were generally 11 to 28 C greater than the cavity temperature, depending upon the flow rate and the wall temperature in the vicinity of the film hole.

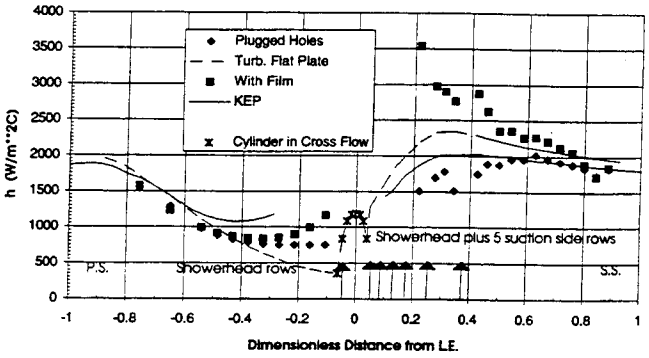

FIGURE 8. Comparison of heat transfer coefficients at an air Reynolds Number of 517,000 with plugged film holes and with film injection through all three film cavities versus the cylinder in cross flow and turbulent flat plate predictions and the boundary layer code (KEP) calculations with no film.

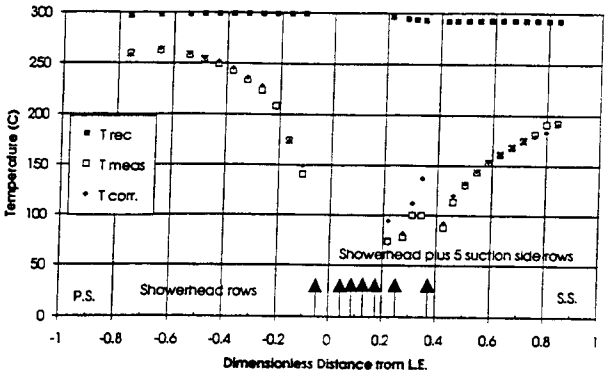

FIGURE 9. Recovery temperature distributions calculated and the steady wall temperatures measured at the end of the transient test at an air Reynolds number of 517,000, with film injection through all the three film cavities.

Considering the airfoil configuration and thermocouple locations, the coolant exit temperature associated with the nearest upstream film row, was used when determining the film effectiveness at each measurement locations. No attempt has been made to predict a mixed film coolant exit temperature due to multiple upstream film rows.

Figure 10 shows the accumulated pressure and suction side raw film effectiveness results with the three film cavities active, for the flow conditions specified above during the transient test. In the same Figure the corrected film cooling effectiveness values are also plotted. The corrections to the measured adiabatic wall temperatures included, conduction corrections calculated on a one-dimensional basis and the measured local heat transfer coefficients.

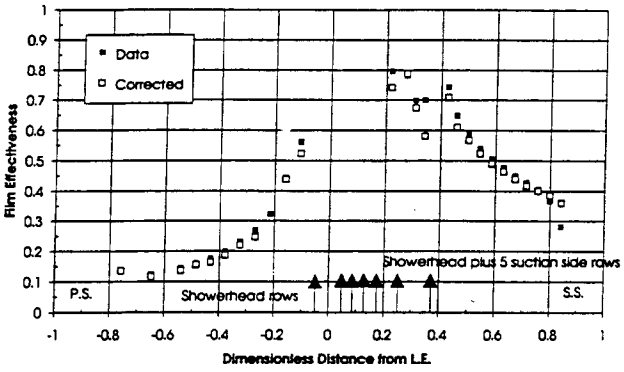

FIGURE 10. Film cooling effectiveness distributions calculated at the end of the transient test at an air Reynolds number of 517,000, with film injection through all the three film cavities.

6. SUMMARY AND CONCLUSIONS

A transient test facility has been built for the purpose of determining both heat transfer coefficient and film cooling effectiveness distributions in a linear airfoil cascade. The cascade is capable of operation in either the steady-state mode, to obtain local adiabatic film effectiveness values, or in the transient mode, to obtain both heat transfer coefficients and film effectiveness values. The transient operation is of particular importance, in that the relevant heat transfer characteristics are determined within the same aero-thermal environment.

A test cascade of cylinders in cross flow has been used to verify the experimental methodology. Stagnation point heat transfer coefficients obtained agree with the established correlation for a cylinder in cross flow including turbulence effects.

Heat transfer coefficient and film cooling effectiveness distributions were obtained for a linear airfoil cascade, with and without film coolant injection at two flow Numbers. For the particular airfoil used in these tests, the findings include i) The pressure and suction side heat transfer coefficients obtained with 14% inlet turbulence and plugged film holes follow the boundary layer code (KEP) predictions, ii) The film injection increases the heat transfer coefficient levels both on the pressure and suction sides.

7. REFERENCES

Abhari, R.S. and Epstein, A.H., 1992, "An Experimental Study of Film Cooling in a Rotating Transonic Turbine," Presented at the International Gas Turbine and Aeroengine Congress and Exposition, Cologne, Germany, June 1992, Paper No. 92-GT-201.

Arts, T. and Lapidus, I., 1992, "Thermal Effects of a Coolant Film Along the Suction Side of a High Pressure Turbine Nozzle Guide Vane," AGARD 80th Symposium of Propulsion and Energetics Panel, Antalya, Turkey, October 1992, AGARD-CP-527.

Camci, C. and Arts, T., 1990, "An Experimental Convective Heat Transfer Investigation Around a Film-Cooled Gas Turbine Blade," Journal of Turbomachinery, Vol. 112, No. 3, pp. 497-503.

Camci, C. and Arts, T., 1991, "Effect of Incidence on Wall Heating Rates and Aerodynamics on a Film-Cooled Transonic Turbine Blade," Journal of Turbomachinery, Vol. 113, No. 3, pp. 493-501.

Dullenkopf, K., Schulz, A., and Wittig, S., 1991, "The Effect of Incident Wake Conditions on the Mean Heat Transfer of an Airfoil," Journal of Turbomachinery, Vol. 113, No. 3, pp. 412-418.

Dunn, M.G. and Stoddard, F.J., 1979, "Measurement of Heat-Transfer Rate to a Gas Turbine Stator," Journal of Engineering for Power, Vol. 101, pp. 275-280.

Dunn, M.G., Kim, J., Civinskas, K.C., and Boyle, R.J., 1992, "Time-Averaged Heat Transfer and Pressure Measurements and Comparison with Prediction for a Two-Stage Turbine," Presented at the International Gas Turbine and Aeroengine Congress and Exposition, Cologne, Germany, June 1992, Paper No. 92-GT-194.

Guenette, G.R., Epstein, A.H., Giles, M.B., Haimes, R., and Norton, R.J.G., 1989, "Fully Scaled Transonic Turbine Rotor Heat Transfer Measurements," Journal of Turbomachinery, Vol. 111, No.1, pp. 1-7.

Haldeman, C.W., Dunn, M.G., MacArthur, C.D., and Murawski, C.G., 1992, "The USAF Advanced Turbine Aerothermal Research Rig (ATARR)," AGARD 80th Symposium of Propulsion and Energetics Panel, Antalya, Turkey, October 1992, AGARD-CP-527.

Harasgama, S.P. and Wedlake, E.T., 1991, "Heat Transfer and Aerodynamics of a High Rim Speed Turbine Nozzle Guide Vane Tested in the RAE Isentropic Light Piston Cascade (ILPC)," Journal of Turbomachinery, Vol. 113, No. 3, pp. 384-391.

Jones, T.V., Schultz, D.L., Oldfield, M.L.G., and Daniels, L.C., 1978, "Measurement of Heat Transfer Rate to Turbine Blades and Nozzle Guide Vanes in a Transient Cascade," 6th International Heat Transfer Conference, Toronto, Canada, Proceedings pp. 73-78.

Kreith, F., 1966, "Principles of Heat Transfer," International Textbook Co., Scranton, PA, pp.408.

Lander, R.D., Fish, R.W., and Suo, M., 1972, "External Heat-Transfer Distribution on Film Cooled Turbine Vane," J. Aircraft, vol. 9, No. 10, pp. 707-714.

Liu, X. and Rodi, W., 1992, "Measurement of Unsteady Flow and Heat Transfer in a Linear Turbine Cascade," Presented at the International Gas Turbine and Aeroengine Congress and Exposition, Cologne, Germany, June 1992, Paper No. 92-GT-323.

Lowery, G.W., and Vachon, R.I., 1975, "The Effect of Turbulence on Heat Transfer From Heated Cylinders," Int. J. Heat and Mass Transfer, vol. 18, pp. 1229-1242.

Mehendale, A.B. and Han, J.C., 1992, "Influence of High Mainstream Turbulence on Leading Edge Film Cooling Heat Transfer," Journal of Turbomachinery, Vol. 114, No. 4, pp. 707-715.

Mehendale, A.B., Han, J.C., and Ou, S., 1991, "Influence of High Mainstream Turbulence on Leading Edge Heat Transfer," J. of Heat Transfer, vol.113, pp. 843-850.

Nirmalan, N.V. and Hylton, L.D., 1990, "An Experimental Study of Turbine Vane Heat Transfer With Leading Edge and Downstream Film Cooling," Journal of Turbomachinery, Vol. 112, No. 3, pp. 477-487.

Ou, S. and Han, J.C., 1992, "Influence of Mainstream Turbulence on Leading Edge Film Cooling Heat Transfer Through Two Rows of Inclined Film Slots," Journal of Turbomachinery, Vol. 114, No. 4, pp. 724-733.

Ou, S., Han, J.C., Mehendale, A.B., and Lee, C.P., 1993, "Unsteady Wake Over a Linear Turbine Blade Cascade With Air and CO2 Film Injection: Part I - Effect on Heat Transfer Coefficients," Presented at the International Gas Turbine and Aeroengine Congress and Exposition, Cincinnati, Ohio, May 1993, Paper No. 93-GT-210 .

Schobeiri, T., McFarland, E., and Yeh, F., 1991, "Aerodynamics and Heat Transfer Investigations on a High Reynolds Number Turbine Cascade," Presented at the International Gas Turbine and Aeroengine Congress and Exposition, Orlando, Florida, June 1991, Paper No. 91-GT-157.

Takeishi, K., Matsuura, M., Aoki, S., and Sato, T., 1990, "An Experimental Study of Heat Transfer and Film Cooling on Low Aspect Ratio Turbine Nozzles," Journal of Turbomachinery, Vol. 112, No. 3, pp. 488-496.

Takeishi, K., Aoki, S., Sato, T., and Tsukagoshi, K., 1992, "Film Cooling on a Gas Turbine Rotor Blade," Journal of Turbomachinery, Vol. 114, No. 4, pp. 828-834.

Vedula, R.J. and Metzger, D.E., 1991, "A Method for the Simultaneous Determination of Local Effectiveness and Heat Transfer Distributions in Three-Temperature Convection Situations," Presented at the International Gas Turbine and Aeroengine Congress and Exposition, Orlando, Florida, June 1991, Paper No. 91-GT-345.

Zerkle, R.D., and Lounsbury, R.J., 1989, "Freestream Turbulence Effect on Turbine Airfoil Heat Transfer," J. Propulsion, vol. 5, No. 1, pp. 82-88.